ISSN: 2710-0588

Research of Defoaming Detection in Shale Foam Drainage Wells Based on Machine Vision

Liang Guo[1, 2, *], Changxu Chen[1], Junhao Wu[1] and Boya Wu[1]

[1]School of Mechatronic Engineering, Southwest Petroleum University, Chengdu 610500, China

[2]Sichuan Shared Platform for Oil and Gas Equipment Technology, Chengdu, 610500, China

[*] Corresponding Author

Abstract

Shale gas is generally faced with the problem of bottom-hole accumulation in the middle and late stage of exploitation. Foam drainage gas production technology is one of the means to solve the problem of bottom-hole accumulation and restore the normal production of gas Wells. When the foam mixture reaches the ground, it needs to be defoamed. At present, the defoaming effect is mainly evaluated by regular manual sampling from the separator sampling port. In order to reduce the work intensity, realize automatic detection and improve the detection accuracy, a set of anti-foam detection system based on machine vision was developed and field test was carried out. The results show that: The defoaming detection system meets the requirements of field conditions, and the system has strong stability and reliability; The defoaming detection model based on DeepLabV3+ has high accuracy, and the processed images are similar to the manual sampling results; The minimum difference between the foam height measurement system and the manual measurement is 0mm, the maximum difference is 8.60mm, and the data with the difference of 5mm and below account for 94.4%, that is, the accuracy rate reaches 94.4%. It is concluded that the development and test of the defoaming detection system has verified the feasibility of using machine vision technology for defoaming detection, and has practical significance for promoting the intelligent development of the defoaming detection process and improving the efficiency of shale gas extraction.

Keywords

Foam drainage gas production; Shale gas; Foam height; Detecting system; Machine vision.

1. Introduction

In the process of shale gas development, the theory of "artificial gas reservoir" is adopted to release shale gas through fracturing technology. If the fracturing fluid is not discharged in time, liquid will form in the wellbore to hinder gas flow, and in serious cases, it may lead to flooding and production suspension[1-3]. In order to solve this problem, it is necessary to adopt drainage gas production technology. Among them, the foam drainage gas production process has become one of the widely used technologies due to its advantages of making full use of the formation's own energy to achieve lifting, low cost, quick response, simple operation and strong adaptability[4-5]. In this process, a large number of low-density water-containing foams are produced by injecting bubble drainage agents into the place where the liquid accumulates or is likely to produce liquid accumulates under the disturbance of air flow. These foams can use the formation's own energy to rise to the surface with the air flow, thereby effectively draining the bottom-hole fluid[6-8]. After the foam fluid reaches the ground, it must be defoamed to achieve effective separation of liquid and gas. Insufficient defoaming will lead to the failure of booster equipment and the deterioration of pipe network performance. Excessive addition of defoamer

ISSN: 2710-0588

increases the cost and the difficulty of wastewater treatment[9-10]. Therefore, in actual operation, it is necessary to determine the appropriate amount of defoamer according to the specific situation of the foam fluid, which requires continuous detection of the defoamer effect in daily production, and dynamic adjustment of the defoamer dosage.

At present, the method of testing the effect of defoaming in the field relies on the operator to collect samples from the sampling port of the separator regularly, observe the foam height after standing, and adjust the filling amount of the automatic filling device of defoaming agent according to the existing evaluation standards. This method is not only time-consuming and laborious, but also increases the work burden of operators due to the wide distribution of gas Wells, and may also have subjective errors. In order to improve inspection efficiency and accuracy, researchers are committed to developing effective wellhead foam detection technology to achieve more accurate management and optimization of defoamer filling. Liang Zheng et al. [11] proposed a variety of anti-foaming effect detection schemes and evaluated their feasibility. Guo Liang et al. [12-13] designed a foam content monitoring device based on the difference in infrared reflectivity, which can distinguish between gas, foam and liquid in the pipeline, and verified its effectiveness and reliability through field tests. Although most of the current research focuses on the use of infrared detection principle for detection, and has achieved certain results, however, with the continuous improvement of detection accuracy and environmental adaptability requirements, infrared methods in some application scenarios gradually show its limitations. Based on this background, this research turns to exploring an innovative solution - using machine vision technology for inspection. This scheme can not only provide more intuitive and detailed image information, but also has higher degree of automation and processing efficiency.

This paper designs and implements a set of wellhead foam defoaming detection system based on machine vision technology, and verifies the feasibility and detection accuracy of the system through field tests. The purpose of this study was to explore the potential of machine vision in improving the efficiency and accuracy of defoaming operations, and to provide a new perspective for defoaming operations in bubble drainage Wells.

2. Architecture of Defoaming Detection System

2.1. Overall test system scheme

Based on the Internet of Things technology, the anti-foam detection system of bubble drainage well adopts a three-layer architecture design, including the perception layer, the transmission layer and the application layer, as shown in Figure 1. First, the sensing layer uses machine vision technology[14] to collect the image of the detection sample through the camera in the defoaming detection device, and uses the Raspberry PI for image processing to accurately measure the foam height. For "one well, one strategy" managed platform Wells, comprehensive inspection can be ensured by equipping each well with an independent sampling device. Secondly, the transport layer realizes wireless data transmission based on 4G cellular network, and securely transmits the image and original image processed by Raspberry PI to the cloud server through HTTP protocol. Finally, in the application layer, the foam height data and the original acquired image obtained from the perception layer are displayed on the Web page in a visual way, and the detection data is stored in the MySQL database to provide a strong basis for the subsequent optimization of the use of defoamer.

ISSN: 2710-0588

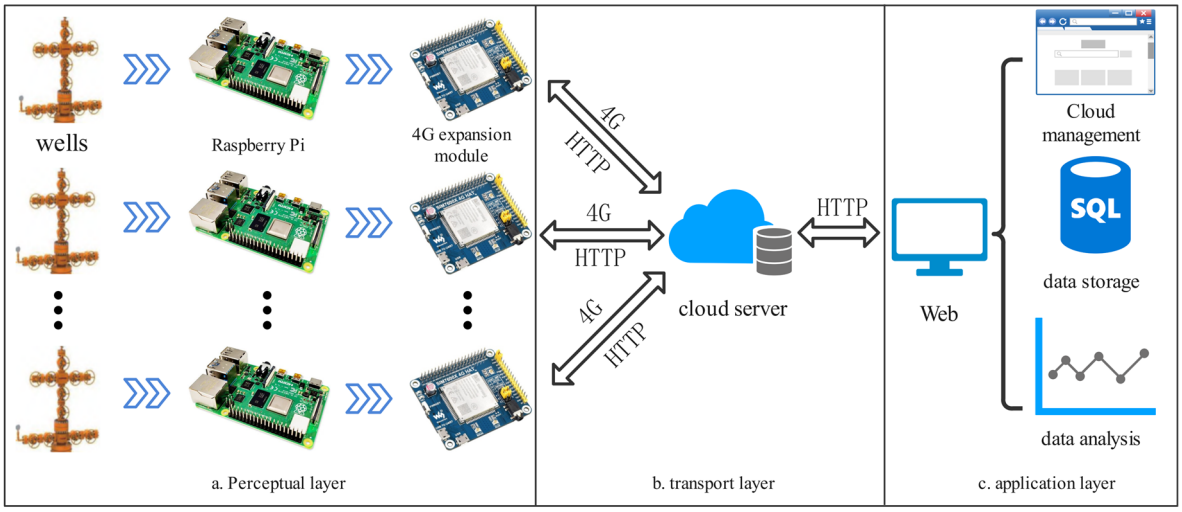

Figure 1. Overall scheme of defoaming detection system at the foam drainage wells

2.2. DeepLabV3+ image semantic segmentation model

According to the evaluation criteria of defoaming effect in the "Management Measures for Bubble Drainage Operation in Southwest Gas Production Plant", the test water sample should be observed after standing for 2 minutes. After standing, the water sample is divided into foam layer and liquid layer. Traditional image processing has problems of insufficient real-time performance and segmentation detail loss in defoaming detection. In order to achieve accurate image recognition of foam height, this study builds a defoaming detection model based on DeepLabV3+, and realizes fine identification of foam layer boundary through codec-decoding architecture and multi-scale feature fusion mechanism[15-16], as shown in Figure 2. In this model, the MobileNetV2 lightweight network is used as the backbone of the encoder, and its deep separable convolution structure can significantly reduce the computational complexity while ensuring the feature extraction capability, and effectively solve the response speed bottleneck in real-time detection scenarios. The encoder first extracts features from the acquired images, which are divided into two parts: one contains shallow features and is transmitted directly to the decoder; The other part is fed into the cavernous space convolution pool Pyramid (ASPP). In order to solve the multi-scale feature extraction problem caused by the dynamic change of foam layer morphology over time, the model introduces the convolution pyramid of void space into the encoder. By setting the convolution layers with expansion rates of 6, 12 and 18 in parallel, the multi-scale semantic features under different receptive fields are captured, and the context information obtained by global average pooling is fused. Form high-dimensional representations that contain both macroscopic and microscopic features. In the decoding stage, the feature pyramid fusion strategy is used to concatenate the high-level semantic features up-sampled by 4x bilinear interpolation with the shallow detailed features optimized by 1×1 convolution channel. After eliminating aliasing effect by 3x 3 convolution, the secondary up-sampling is restored to the original resolution. Finally, based on the pixel-level segmentation results, the spatial mapping model of image pixel coordinates and beaker calibration scale is established to accurately calculate the actual height of the foam layer. The distribution of foam layer is visually displayed by false color overlay visualization technology, which provides reliable technical support for the evaluation of defoaming effect.

ISSN: 2710-0588

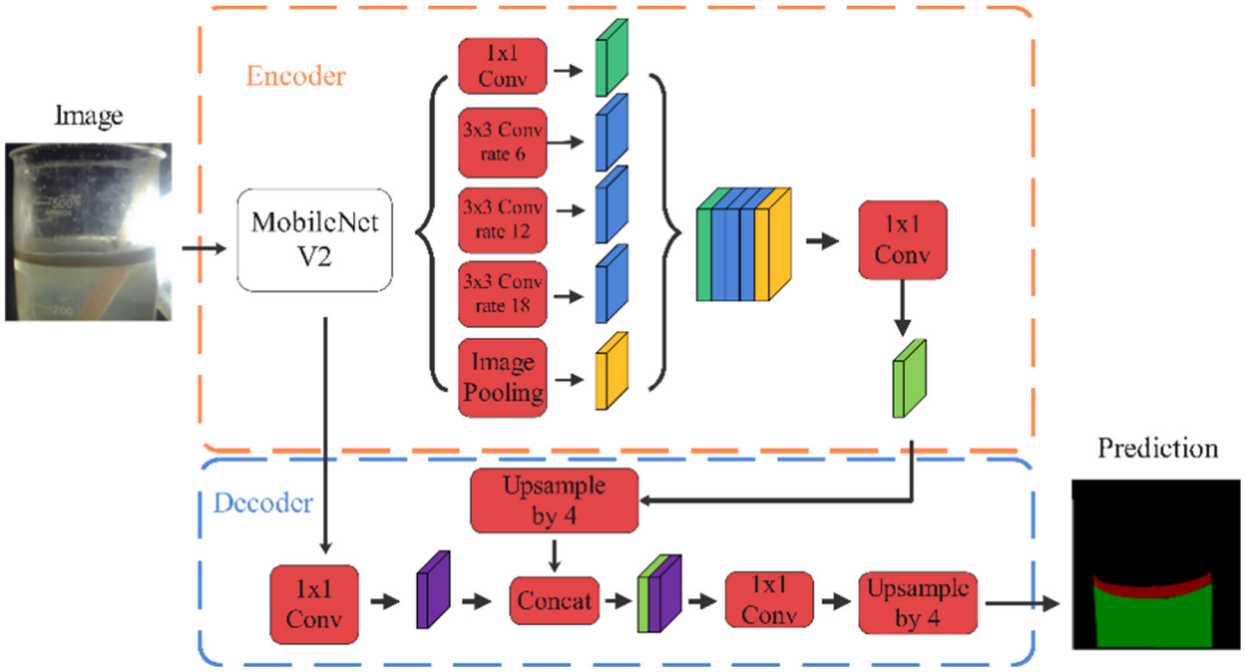

Figure 2. DeepLabV3+ network model

2.3. Detection device scheme

The modular antifoam testing system designed according to the actual working condition of the site adopts the layered structure design, which is divided into three layers: upper, middle and lower. FIG. 3 shows the device diagram of the defoaming detection system. The upper layer is equipped with electronic component modules including Raspberry PI, transformer, 4G expansion board (SIM7600X), MOS field effect and relay; The middle layer is equipped with a sampling assembly composed of an electric ball valve, a one-way throttle valve, a connecting pipe and corresponding connecting accessories, which are placed in the same explosion-proof box and isolated from the upper layer by explosion-proof mud and insulation board; The lower level is used for image acquisition and contains the camera, light source, sampling beaker and liquid discharge pump, which are arranged in two separate explosion-proof chambers. When the system is running, through the pre-set one-way throttle opening, when the collection command is received, the Raspberry PI starts the relevant procedures, the electric ball valve opens in response, and the foam mixture flows into the sampling beaker. Then, after standing for a period of time according to the anti-foam evaluation standard, the light source in the lower layer is turned on, the camera takes images and transmits data, and finally the liquid in the sampling beaker is discharged through the drainage pump to complete a single collection. Because of its small size, economy and easy development, Raspberry PI serves as the control core in this study, which is used to realize the operation of the detection device according to the preset program and image processing of the collected data. It then transmits the processed image and resulting data to a Web page for real-time monitoring and analysis. In addition, the device adopts the USB camera module suitable for the Raspberry PI Linux system and the normally closed electric ball valve to ensure the safety and convenience of operation. At the same time, the light source and the camera are distributed at a 120° Angle, and the light source is 10cm away from the beaker to achieve the best detection effect.

ISSN: 2710-0588

Figure 3. Device diagram of defoaming detection system

3. Laboratory Experiment

3.1. Experimental flow scheme

Based on DeepLabV3+ network model, an experimental flow of foam height detection is designed. First, a laboratory test is conducted using a detection device to obtain foam images and build a data set. The data set is divided into the training set and the validation set in a ratio of 9:1. The training set is used to train the defoaming detection model to achieve effective separation of foam layer and liquid layer, and the stability and accuracy of the model are evaluated by validation set. After the foam layer is divided, the edge of the foam layer is determined by pixel marking method. Finally, the final foam height is obtained by converting the pixel distance in the image into the actual distance.

3.2. Data set construction

Labelme labeling tool was used to label the foam image, and the region in the image was divided into foam layer and liquid layer labels. When this is done, the saved image and the resulting json file are converted to a dataset containing the original image and labels by the json_to_dataset conversion tool. In the laboratory experiment, a total of 600 images, covering different foam heights and beaker cleanliness, were produced and labeled to complete the construction of the dataset.

3.3. Experimental Measurement

The data set is divided into the training set and the validation set in a ratio of 9:1. By means of transfer learning, the weights pre-trained on ImageNet data set are used to initialize the model, accelerate the training speed and improve the performance. Hardware configuration includes Intel Core i5-9300H CPU and NVIDIA GeForce 1650 GPU, software environment Windows10 system, running PyTorch1.9.0+Python3.8. The models were trained with 50 epochs, a batch size of 8, an SGD optimizer, an initial learning rate of 0.007, and a cross-entropy loss function.

The model was trained according to the above configuration parameters, and two semantic segmentation indexes, namely mean pixel accuracy (mPA) and mean crossover ratio (mIoU), were used to evaluate the model performance[18]. The results of mIoU experiment were 96.93% and mPA experiment 98.71%, indicating a high accuracy.

3.4. Experimental results and analysis

The traditional image processing and deep learning detection methods are compared, and foam images with clean and impurities are selected. As shown in Figure 4, the results obtained by the above two methods are partially clean beakers and beakers with impurities interference. It can be seen that when the inner wall of the beaker is clean and tidy and there is no interference of impurities, the two methods can detect the edge of the foam layer more accurately. When the

ISSN: 2710-0588

inner wall of beaker is polluted with impurities, the traditional image processing method has poor effect on the edge recognition of foam layer. The results show that the deep learning method can accurately identify the boundary of the foam layer, indicating that the defoaming detection model based on DeepLabV3+ network has high reliability and accuracy in defoaming detection.

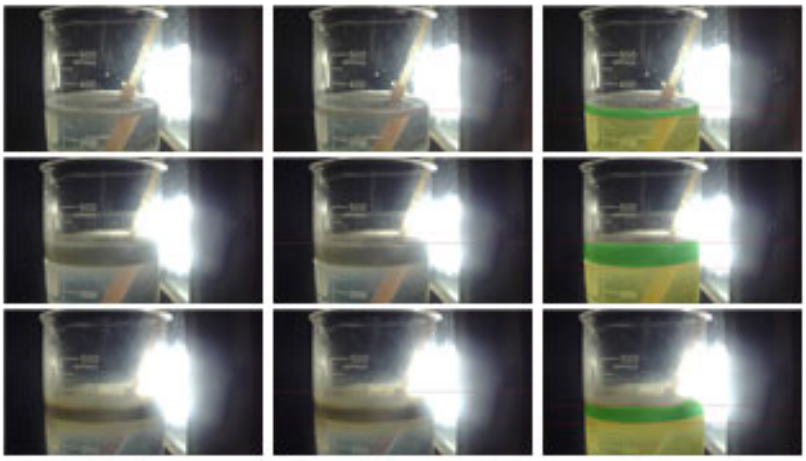

Figure 4. Comparison of experimental results

4. Field Experimentation

4.1. Test process and results

The field test process was designed according to the field blister operation system. Since electronic equipment is prohibited in the open air environment of the gas production site, all tests should be assisted by two groups AB. Group A is located at the sampling point and is responsible for manual sampling and confirming the operating status of the detection device. Group B is located in the RTU control cabinet and is responsible for monitoring the normal operation of the system and model optimization. Specific experimental steps are as follows:

1) Team B in the RTU control cabinet starts the testing procedure and records the relevant data, and indicates Team A in the RTU control cabinet to take samples through beakers;

2) After the completion of sampling, set the sampling beaker to rest. After 2 minutes, the staff of Group B in the RTU control cabinet shall signal the staff of Group A in the RTU control cabinet to complete the reading and record the foam height sampled by the beaker;

3) Wait for the next sampling instruction from Group B of RTU control cabinet;

4) Repeat the above test steps 1-3;

5) Extract the foam height data obtained by the detection system and make a comparative analysis with the manual sampling records.

4.2. Interpretation of result

1) Trend analysis of system detection and manual measurement data

Through the statistical analysis of 180 groups of foam height data from the detection system and the foam height data recorded by manual sampling, the comparison curve is obtained. It can be seen that the trend of foam height data obtained by the detection system is basically the same as that obtained by manual sampling, indicating that the detection system can accurately

ISSN: 2710-0588

reflect the actual situation on the site and the detection system is feasible. The statistical curve between the detection system and the manual detection of foam height is shown in Figure 5.

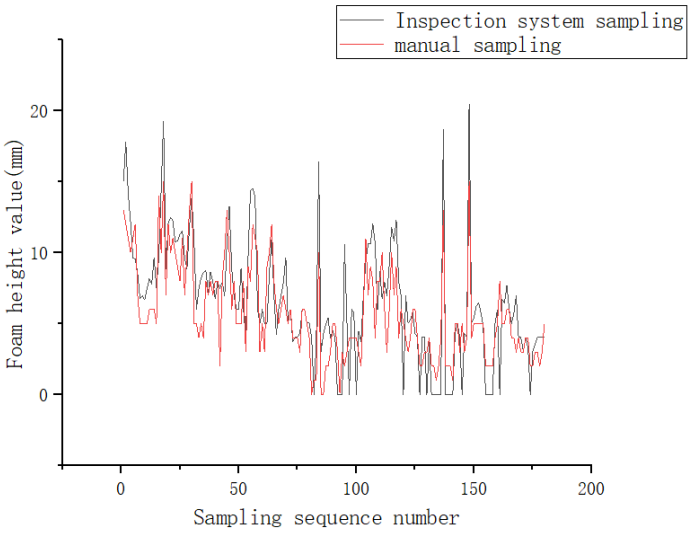

Figure 5. Statistical curve of foam height between detection system and manual sampling

2) Analysis of the difference between system detection and manual measurement data

In order to further evaluate the accuracy of the detection system, the difference between the foam height sampled by the detection system and the foam height data obtained by manual sampling was analyzed. If the difference between the detection system and the manual detection is less than 5mm, it is considered that the detection system value can approximately replace the manual detection. The difference curve of foam height between the detection system and manual detection is shown in Figure 6. As can be seen from the figure, the minimum height difference of the foam layer is 0mm, and the maximum height difference is 8.60mm. Among them, there are 170 groups of data whose height difference of the foam layer is 5mm or below, accounting for 94.4% of the total sample. According to the evaluation criteria of the field defoaming effect, the detection is considered accurate if the difference of foam height is controlled within 5mm or below. As a result, the accuracy of the detection system was 94.4%.

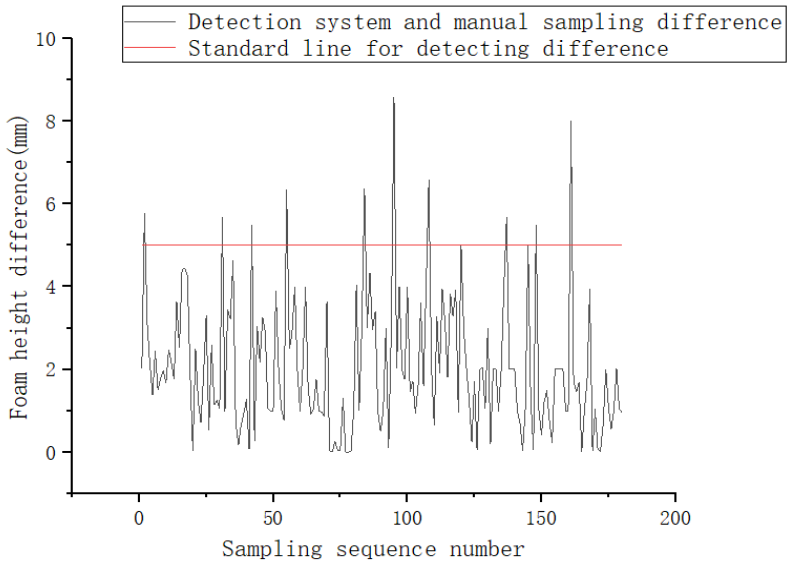

Figure 6. Difference curve of foam height between detection system and manual sampling

ISSN: 2710-0588

5. Conclusion and Suggestion

1) The developed antifoam detection system has no mechanical failure, good sealing performance, meets the requirements of on-site explosion-proof, stable data transmission, and real-time data results are displayed at the front end, meeting the actual operating conditions.

2) The defoaming detection model based on DeepLabV3+ can effectively achieve image segmentation between foam layer and liquid layer and accelerate the response speed of obtaining detection results. The results show that the mIoU and mPA of the model are 96.83% and 98.71% respectively, which proves that the model has high accuracy.

3) Field tests were carried out and 180 sets of data collected were analyzed. The results showed that the minimum difference between the system detection and manual measurement of foam height was 0mm, and the maximum difference was 8.60mm. The proportion of data with a difference of 5mm or less was 94.4%, that is, the accuracy rate reached 94.4%, and the detection accuracy was high.

References

[1] ZHAO Kang, CHEN Minfeng, WANG Yiwen, et al. Production decline rule and recoverable reserves prediction of TY water-bearing shale gas reservoir[J] Fault-Block Oil & Gas Field, 2024, 31(3):395-402.

[2] CHEN Chao, CHEN Xuezhong, CHEN Man, et al. Research and application of intelligent integrated composite drainage and production process system for shale gas wells[J]. Fault-Block Oil & Gas Field, 2024, 31(6):1129-1136.

[3] CHEN Xiaolu, LYU Zhenhu, LU Zongyu, et al. Research and application of key technologies for volume fracturing of deep tight conglomerate reservoirs in Mahu Oilfield[J]. Fault-Block Oil & Gas Field, 2024, 31(6):1098-1104.

[4] JIANG Yixin, LIU Cheng, GAO Haohong, et al. Foam drainage gas recovery technology and its application in the shale gas wells of Zhaotong National Shale Gas Demonstration Area[J]. Natural Gas Industry, 2021, 41(S1): 164-170.

[5] FEI Haihong. Technique of Gas Recovery by Water Drainage for Zhujiadun Gas Pool in Yancheng, Jiangsu[J]. Fault-Block Oil & Gas Field, 2006, (6):73-75+93-94.

[6] ZHAI Zhongbo, CHEN Gang, ZHU Zhixian, et al. Onset time of lift-assisted foam drainage gas recovery in adjacent wells [J]. Natural Gas Exploration and Development, 2024, 47(2): 68-72.

[7] LI Jiaxin, ZHANG Ningbo, ZHOU Chengxiang. Application of foam drainage-gas recovery technology in shale gas wells: A case study of southern Pingqiao[J]. Reservoir Evaluation and Development, 2020, 10(5):91-97.

[8] QU Chaochao, LIU Zhengzhong, YIN Hongyao, et al. A new anti-condensate foaming agent for drainage gas recovery[J]. Acta Petrolei Sinica, 2020, 41(7): 865-874.

[9] HAN Yong, GAO Shiju, MOU Chunguo, et al. Optimization research of the solid defoaming process in Sulige Field[J]. Drilling and Production Technology, 2020, 43(6): 62-64.

[10] JIANG Zeyin, LI Wei, LUO Xin, et al. Foam drainage gas recovery technology for shale-gas platform wells[J]. Natural Gas Industry, 2020, 40(4): 85-90.

[11] LIANG Zheng, DENG Xiong, LV Zhizhong, et al. Project design of monitoring system of defoaming effect for foaming drainage gas recovery[J]. Oil Field Equipment, 2009, 38(8): 17-20.

[12] ZHENG Rui, LIANG Jing, LI Ying, et al. The cloud monitoring system of wellhead foam content used for foam drainage gas recovery wells[J]. Natural Gas Industry, 2021, 41(S1): 171-176.

[13] GUO Liang, WANG Ruiyu, CHENG Changxu, et al. Application of foam content monitoring system in foam drainage shale gas wells[J]. Natural Gas Industry, 2023, 43(12): 63-70.

[14] ZHANG Jinsong, QU Zhe, YUE Mengkun, et al. Machine vision system for high-temperature wind tunnel: Principle, design and application(in Chinese). Sci Sin Tech, 2020, 50(6):742-762.

ISSN: 2710-0588

[15] WU Jinlong, WU Hongqi, LI Hao, et al. Segmentation of Buckwheat by UAV Based on Improved Lightweight DeepLabV3+ at Seedling Stage[J]. Transactions of the Chinese Society for Agricultural Machinery, 2024, 55(5):186-195.

[16] HU Jinwei, XI Zhenghao, XU Guozhong, et al. An improved automated testing model for maceral groups in coals based on DeeplabV3+[J]. Coal Geology & Exploration, 2023, 51(10):27-36.

[17] FANG Jiaji, LAI Yibo, TANG Zhengtao, et al. Lightweight power line semantic segmentation method based on DeepLabv3+[J]. Computer Era, 2023, (9):19-23+28.

[18] JING Zhuangwei, GUAN Haiyan, PENG Daifeng, et al. Survey of research in image semantic segmentation based on deep neural network[J]. Computer Engineering, 2020, 46(10):1-17.